Effect of spacer groups on the performance of MCM-41-supported platinum cluster-derived hydrogenation catalysts

Niladri Maity [a], Susmit Basu [a], Maitri Mapa [c], Pattuparambil R. Rajamohanan [d], Subramanian Ganapathy [d], Chinnakonda S. Gopinath [c], Sumit Bhaduri [b,*], Goutam Kumar Lahiri [a,*]

[a] *Department of Chemistry, Indian Institute of Technology–Bombay, Powai, Mumbai 400076, India*
[b] *Reliance Industries Limited, Swastik Mills Compound, V.N. Purav Marg, Chembur, Mumbai 400071, India*
[c] *Catalysis Division, National Chemical Laboratory, Pune 411008, India*
[d] *Central NMR Facility, National Chemical Laboratory, Pune 411008, India*

Abstract

MCM-41 was functionalized with $(EtO)_3SiCH_2Cl$, $(MeO)_3SiCH_2CH_2CH_2Cl$, and $(CH_3)Cl_2SiCH_2Cl$. The functionalized materials were characterized by solid-state NMR (CPMAS, ^{29}Si and ^{13}C) and XPS. The NMR data indicate that three new silicon environments were created by $(EtO)_3SiCH_2Cl$ and $(MeO)_3SiCH_2CH_2CH_2Cl$, whereas with $(CH_3)Cl_2SiCH_2Cl$, two new silicon environments were obtained. XPS results from Si 2*p* core level and the valence band from the material functionalized by $(MeO)_3Si(CH_2)_3Cl$ was found to be the same as that of the corresponding fresh catalyst (**1a**), in contrast to that of the materials functionalized by the other two silane reagents. After further functionalization with triethylamine, these materials were used as inorganic anion exchangers to support the cluster anion $[Pt_{12}(CO)_{24}]^{2-}$. Solid-state NMR (^{29}Si, ^{13}C, ^{15}N) was used to establish the presence of the quaternary ammonium group in the cluster-supported species. Analogous materials were also created using fumed silica as the support, and all of the cluster-supported materials were tested as catalysts for the hydrogenation of methyl pyruvate, acetophenone, nitrobenzene, benzonitrile, ethylacetoacetate, 4-nitrotoluene, cyclohexanone, allyl alcohol, and styrene. The best activity was obtained for the catalyst that had MCM-41 as the support and chloropropyl as the spacer group. TEM showed that the supports and the spacer groups had observable effects on the platinum crystallite size of the catalysts.

Keywords: Platinum carbonyl cluster; Hydrogenation catalysts; Functionalized inorganic oxides; Spacer groups; Solid-state NMR; XPS; MCM-41

1. Introduction

A common method for preparing polymer-supported homogeneous catalysts involves the tethering of a pendant ligand onto an insoluble polymer support. Such catalysts are useful because they can be separated from the reaction mixture by simple filtration [1–7]. With inorganic oxides (e.g., silica gel, MCM-41), reactions with suitable silane reagents are widely used as the first step toward functionalization of the support [8].

The reaction of silica-based materials (e.g., silica gel, MCM-41) with (3-chloropropyl)trimethoxysilane [i.e., $(MeO)_3SiCH_2CH_2CH_2Cl$] is a common method for the initial functionalization of the support [8–10]. Once thus functionalized, the chloropropyl group can be converted to the desired ligands by conventional methods of synthetic organic chemistry. This strategy has been used to functionalize MCM-41, and mainly one type of surface site, as shown by **1′** (Scheme 1), has been implicitly assumed to be present [11–13].

The work reported herein was undertaken with the three objectives in mind. The first objective was to functionalize MCM-41 by different chloroalkylsilanes and characterize the surface sites. To achieve this, apart from $(MeO)_3SiCH_2CH_2CH_2Cl$, two other silicon reagents, $(EtO)_3SiCH_2Cl$ and $(CH_3)Cl_2SiCH_2Cl$, were reacted with MCM-41. The resultant materials **1′**, **2′**, and **3′** (see Schemes 1 and 2) were characterized by solid-state NMR (^{29}Si and ^{13}C CPMAS) and XPS.

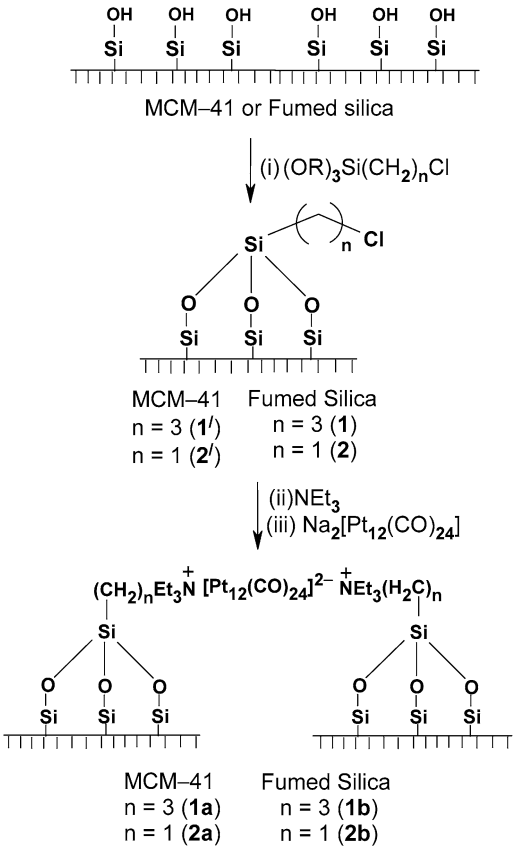

Scheme 1. Synthetic procedure for preparation of **1a** to **2b**.

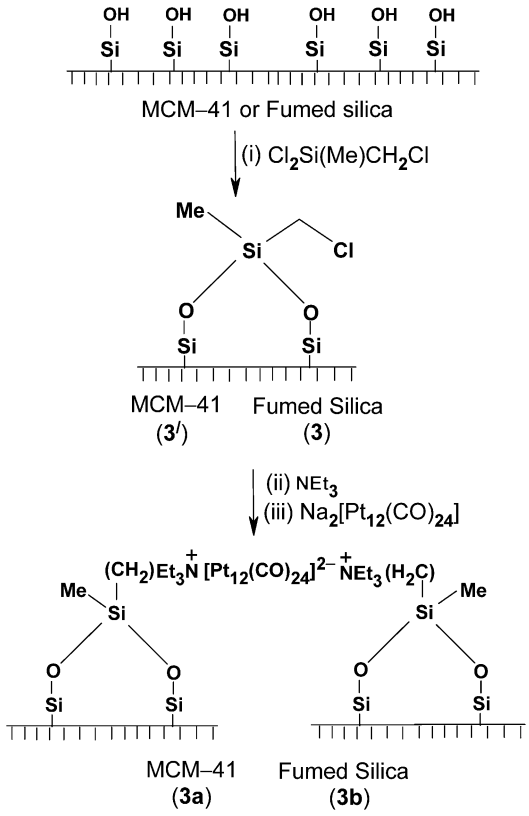

Scheme 2. Synthetic procedure for preparation of **3a** and **3b**.

The second objective was to determine the effect of the pendant chloroalkyl functionality and the inorganic silica support on catalytic properties. To meet this objective, the functionalized materials were used to prepare platinum cluster-derived hydrogenation catalysts by a procedure reported previously by us [13,14]. This method involves using triethylamine and the Chini cluster $[Pt_{12}(CO)_{24}]^{2-}$ in a sequential manner after silylation, as shown schematically in Schemes 1 and 2. To determine whether the regular pore structure of MCM-41 results in higher activities, analogous catalysts were also prepared using fumed silica as the support. The six precatalysts, formulated as **1a**–**3b**, were then used to hydrogenate various unsaturated substrates, and their activities were compared.

Finally, the treatment of MCM-41 with $(MeO)_3SiCH_2CH_2CH_2Cl$ is known to lead to the generation of multiple surface sites that can be formulated as $(–O–)_nSi(OMe)_{3-n}CH_2CH_2CH_2Cl$ ($n = 1$–3) [9,15]. The third objective was to investigate the nature of the surface sites in the final catalyst by multinuclear solid-state NMR (^{29}Si, ^{13}C, and ^{15}N). This is important because up to now, the presence of quaternary ammonium groups has been assumed but not proven directly [11,13,14].

2. Experimental

All preparations and manipulations were performed using standard Schlenk techniques under an nitrogen atmosphere. Solvents were dried by standard procedures (i.e., toluene over Na/benzophenone; methanol over Mg-turnings/iodine), distilled under nitrogen, and used immediately. Chloroplatinic acid was purchased from Johnson Mathey. Methyl pyruvate, methyl lactate, cinchonidine, and colloidal silica and benzylamine were purchased from Fluka. Fumed silica, (3-chloropropyl)trimethoxysilane, chloromethyldichloromethylsilane, chloromethyltriethoxysilane, 1-phenylethanol, triethylamine, 3-hydroxybutyrate, allyl alcohol, styrene, and acetophenone were obtained from Aldrich. Benzonitrile and ethylacetoacetate were purchased from Spectrochem. Nitrobenzene, aniline, cyclohexanone, and 4-nitrotoluene were obtained from Merck. MCM-41 and $Na_2[Pt_{12}(CO)_{24}]$ were synthesized as described previously [16,17]. All of the hydrogenation reactions were carried out in an autoclave. Conversions in the hydrogenation reactions with different substrates were monitored using a gas chromatograph with a flame ionization detector (Shimadzu GC-14A) and a capillary column (CBP20-M-25-025, Shimadzu capillary column; 25 m long, 0.25 μm i.d., 0.20 mm film). All hydrogenated products were initially identified using authentic commercial samples of the expected products. Thermo Nicolet 320 FT-IR and Jasco V-570 UV–vis spectrophotometers were used for recording IR and reflectance spectra, respectively. Microanalytical experiments were carried out using a CE Instruments, Flash EA 1112 Series (Thermo Quest) CHN analyzer. An FEI Quanta 200 instrument (using tungsten filament as source for the electron beam and a gaseous secondary electron detector) was used for ESEM and EDAX analysis. A JEOL 1200 EX transmission electron microscope was used for the surface analysis of catalysts. XPS studies were done with a VG Microtech Multilab XPS 3000 instrument.

Solid-state ^{13}C, ^{29}Si, and ^{15}N spectra were obtained on a Bruker DRX 500 NMR spectrometer operating at 125.75, 99.35, and 50.68 MHz, respectively, using a broad-band CP-MAS probe. Samples were spun at 8 or 10 kHz using 4-mm zirconia rotors. Bloch decay spectra were acquired using a 30-degree flip angle (2 μs) excitation pulse and a 2 s relaxation delay, under ^{1}H decoupling at an applied radio frequency field of 45 kHz to improve ^{29}Si signal resolution. ^{29}Si, ^{13}C, and ^{15}N CPMAS spectra were acquired under Harmann–Hahn matching at applied radiofrequency fields of 36 kHz (^{29}Si) and 41 kHz (^{13}C, ^{15}N), using contact times of 5 ms (^{29}Si, ^{15}N) and 1 ms (^{13}C) and relaxation delays of 4 s (^{29}Si) and 2 s (^{13}C, ^{15}N). Typically, 15,000–20,000, 8000–15,000, and 29,000 transients were collected for the ^{29}Si, ^{13}C, and ^{15}N experiments, respectively. The ^{13}C chemical shifts were referred to the methine carbon (29.46 ppm) of adamantine and neat tetraethylorthosilicate (−82.4 ppm) was used as the reference of ^{29}Si. The ^{15}N chemical shift was referred to solid NH_4Cl (0 ppm). The liquid-state measurements of the neat silane reagents were carried out using a standard 5-mm broadband inverse probe.

2.1. Functionalization of fumed silica

Fumed silica was dried at 200 °C under vacuum for 24 h. Dried fumed silica (1 g) was treated with neat (3-chloropropyl)trimethoxysilane (15 mL) at 110 °C in an oil bath for 96 h. It was then filtered and washed thoroughly using toluene followed by methanol. On functionalization initial white color of the solid support changed to yellow. The same procedure was also adopted to functionalize the fumed silica by other two silicon reagents, chloromethyldichloromethylsilane and chloromethyltriethoxysilane.

2.2. Functionalization of MCM-41

MCM-41 (1 g) preheated under vacuum at 200 °C for 4 h was refluxed with 2 mL of (3-chloropropyl)trimethoxysilane and 20 mL of dry toluene at 110 °C for 160 h. The product was then separated by filtration and washed several times with dry toluene. Similarly, MCM-41 was also functionalized by using the other two silanes, chloromethyldichloromethylsilane and chloromethyltriethoxysilane.

2.3. Modification of functionalized fumed silica and MCM-41 by triethylamine

The functionalized MCM-41 [functionalized by (3-chloropropyl)trimethoxysilane or chloromethyldichloromethylsilane, or chloromethyltriethoxysilane] (1 g) and freshly distilled triethylamine (10 mL) were added in dry toluene (10 mL). The mixture was heated to reflux at 110 °C for 96 h. It was then filtered and washed thoroughly with dry toluene followed by dry methanol. The same procedure was adopted for the modification of functionalized fumed silica.

2.4. Synthesis of catalysts *1a–3b*

Dried triethylamine modified functionalized support (MCM-41 or fumed silica) (1 g) was added in preformed green methanolic solution (15 mL) of $Na_2[Pt_{12}(CO)_{24}]$ (0.2 g) under carbon monoxide atmosphere. The mixture was stirred at 25 °C for 48 h (for MCM-41) and 96 h (for fumed silica). The solid material was filtered off and washed thoroughly with dry methanol and then dried under CO atmosphere. The specific surface areas (m^2/g) of **1a**, **2a**, and **3a** were 630, 650, and 710, respectively. The pore size distributions of pores of 1–20 Å in terms of relative volume (%) in **1a**, **2a**, and **3a** were 93, 94, and 93, respectively. The specific surface area (m^2/g) of **1b**, **2b**, and **3b** were 180, 210, and 290, respectively.

2.5. Thermal activation of catalysts *1a–3b*

The catalyst **1a–3b** (1 g) was taken in a three-necked round-bottomed flask (25 mL) equipped with nitrogen and vacuum adapters and was flushed with nitrogen to remove any residual oxygen. The system was evacuated and then heated at 70 °C for 4 h under a continuous flow of hydrogen gas. This gray material thus obtained was used in catalytic experiment with suitable substrates.

2.6. Catalytic experiments with activated catalysts *1a–3b*

The catalytic runs in general were carried out at 27 or 70 °C with specified amounts of catalysts and substrates in fixed volumes of methanol in glass vials. The glass vial was placed in an autoclave, and hydrogen pressure of 50 bar was applied. At the end of the catalytic run, the reaction mixture was subjected to GC, and the extent of conversion was calculated on the basis of the ratio of areas of starting material and the product. More details are given in Tables 1–3.

3. Results and discussion

3.1. Characterization of *1′*, *2′*, and *3′* by solid-state NMR, XPS, and TEM

There are many reports on the use of solid-state NMR (MAS and/or CPMAS) for the characterization of surface functionalized silica in general and chloropropyl functionalized MCM-41

Table 1
Turnover numbers (TON) at 27 °C for ketonic substrates and benzonitrile

Catalysts	Substrates			
	Methyl pyruvate	Ethylacetoacetate	Benzonitrile	Acetophenone
1a	72	51	48	50
2a	47	29	21	40
3a	45	20	3	16
1b	55	35	44	43
2b	27	18	12	18
3b	45	15	22	40

Note. TON = mmol of product/mmol of platinum. All catalytic runs carried out with 70 mg of **1a–3b** (1.6×10^{-2}, 1.8×10^{-2}, 1.8×10^{-2}, 2.0×10^{-2}, 1.5×10^{-2}, and 1.8×10^{-2} mmol platinum, respectively), and 120 mg of substrate (1.17, 0.92, 1.16, and 0.99 mmol of methyl pyruvate, ethylacetoacetate, benzonitrile, and acetophenone, respectively) in 2 mL methanol under a hydrogen pressure of 50 bar. Duration of reaction is 6 h for methyl pyruvate, and 20 h for the others.

Table 2
Turnover numbers (TON) of ketonic substrates with higher amounts of substrate and/or at higher temperature

Catalysts	Substrates			
	Cyclohexanone	Methyl pyruvate	Ethylacetoacetate	Acetophenone
1a	3360	1460	1150	1200
2a	190	1050	390	420
3a	95	870	490	410

Note. TON = mmol of product/mmol of platinum. All the catalytic runs were carried out with 70 mg of **1a**, **2a**, and **3a** (1.6×10^{-2}, 1.8×10^{-2}, and 1.8×10^{-2} mmol platinum, respectively) in 10 mL methanol under a hydrogen pressure of 50 bar. The amounts of substrate used were 8.4 g (85.59 mmol) of cyclohexanone and 2.4 g of methyl pyruvate, ethylacetoacetate, and acetophenone (23.50, 18.44, and 19.97 mmol, respectively). The reaction temperatures were 27 °C for cyclohexanone and 70 °C for all the others. Duration of reaction is 6 h for cyclohexanone and methyl pyruvate, and 20 h for ethylacetoacetate and acetophenone.

Table 3
Turnover numbers (TON) of benzonitrile, nitroaromatics and substrates with alkene functionalities with higher amounts of substrate and/or at higher temperature

Catalysts	Substrates				
	Benzonitrile	Nitrobenzene	4-Nitrotoluene	Styrene	Allyl alcohol
1a	1450	4030	3690	4830	32,190
2a	90	3580	1960	2010	24,890
3a	170	3550	2770	3130	26,610

Note. TON = mmol of product/mmol of platinum. All catalytic runs carried out with 70 mg **1a**, **2a**, and **3a** (1.6×10^{-2}, 1.8×10^{-2}, and 1.8×10^{-2} mmol platinum, respectively) under a hydrogen pressure of 50 bar. Amounts of substrate used were 2.4 g of benzonitrile (23.27 mmol), 8.4 g of nitrobenzene, 4-nitrotoluene, and styrene (68.23, 61.25, and 80.65 mmol, respectively), and 30 g allyl alcohol (516.52 mmol) in 10 mL methanol. Reaction temperatures were 70 °C for allyl alcohol and benzonitrile and 27 °C for all the other substrates. Duration of reaction is 20 h for benzonitrile, 6 h for nitrobenzene, 4-nitrotoluene, and allyl alcohol, and 4 h for styrene.

in particular [15,18–20]. Based on such studies, more than one type of surface structure has been reported in the literature for both chloropropylated silica gel and MCM-41 [9,10,15]. However, for clarity, in Schemes 1 and 2, only one type of surface site corresponding to each silane reagent is shown.

The NMR spectrum of MCM-41 (^{29}Si, MAS, and CPMAS) used by us shows peaks attributable to Q^4, Q^3, and Q^2 silicon [$Q^n = Si(OSi)_n(OH)_{4-n}$ by convention]. The positions of the signal (Figs. 1a and 1e) at $\delta = -110.5$, -102.1, and -92.4 are very similar to the values reported in the literature [9]. The apparent increase in spectral resolution is attributable to the increased B_0 field that we have used (11.7 T) over that reported earlier (9.4 T).

As shown in Figs. 1d and 1h, after reaction with $(CH_3O)_3SiCH_2CH_2CH_2Cl$, the intensities of the Q^3 and Q^2 signals of MCM-41 are substantially reduced, and three new signals of approximately 2:3:2 intensity ratios at $\delta = -50.2$, -59.0, and -68.2 are observed. It is well known that in CPMAS spectra, the intensities of the signals are not proportional to their concentrations. Thus the intensity ratios are calculated from the MAS spectra, in which they can be clearly seen. These chemical shifts are very close to the reported values for T^1, T^2, and T^3 [$T^m = R\,Si(OSi)_m(OMe)_{3-m}$ by convention] silicon, that is, formulations **C**, **B**, and **A**, respectively (see Fig. 2).

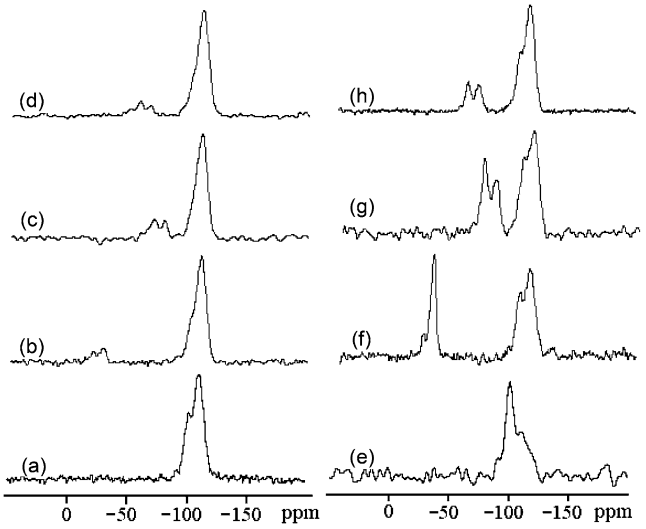

Fig. 1. ^{29}Si MAS (a–d) and CPMAS (e–h) spectra. (a, e) MCM-41; (b, f) MCM-41 functionalized by $(CH_3)Cl_2SiCH_2Cl$; (c, g) MCM-41 functionalized by $(C_2H_5O)_3SiCH_2Cl$; (d, h) MCM-41 functionalized by $(CH_3O)_3SiCH_2CH_2CH_2Cl$.

Fig. 3 shows the ^{13}C spectra of MCM-41 after its reaction with the three silane reagents. For the $(CH_3O)_3SiCH_2CH_2CH_2Cl$-derived material we see three ^{13}C resonances at 9.4, 26.4, and 46.6 ppm. These chemical shifts are again very close to the reported chemical shifts (carbon denoted in italics) of $Si(OMe)_nCH_2CH_2CH_2Cl$, $Si(OMe)_nCH_2CH_2CH_2Cl$, and $Si(OMe)_nCH_2CH_2CH_2Cl$ functionalities, respectively [9]. The signal due to $Si(OCH_3)_nCH_2CH_2CH_2Cl$ is not fully resolved and appears as a shoulder at 50.1 ppm.

The material derived from the reaction of MCM-41 with $(EtO)_3SiCH_2Cl$ shows three silicon signals (Figs. 1c and 1g) at -79.6, -69.7, and -60.2 ppm, attributable to formulations **A**, **B**, and **C**, (i.e., T^3-, T^2-, and T^1-type functionalized environments), respectively. In the MAS spectra, the T^1 signal is much weaker than the other two signals, indicating that the relative amount of **C** for this material is much less than that of **A** and **B.** Three ^{13}C resonances at 59.5, 23.2, and 16.5 ppm are observed in the ^{13}C CPMAS spectrum (Figs. 3b and 3e) for $Si(OCH_2CH_3)_nCH_2Cl$, $Si(OCH_2CH_3)_nCH_2Cl$, and $Si(OCH_2CH_3)_nCH_2Cl$, respectively.

^{29}Si MAS/CPMAS for the material derived from the reaction of MCM-41 with $(CH_3)Cl_2SiCH_2Cl$ shows two functionalized environments with silicon chemical shifts at -30.0 and -20.7 ppm (Figs. 1b and 1f). These signals are considerably deshielded with respect to the MCM-41 and are ascribed to species of types **D** and **E**. Taking into account that for both $(CH_3O)_3SiCH_2CH_2CH_2Cl$- and $(EtO)_3SiCH_2Cl$-functionalized MCM-41, the concentration of the T^2 environment is greater than that of the T^1 environment, the stronger signal at -30.0 ppm is attributed to species **D** and that at -20.7 ppm is attributed to species **E**. Two ^{13}C resonances at 27.6 and -6.1 ppm are observed in the ^{13}C CPMAS spectrum

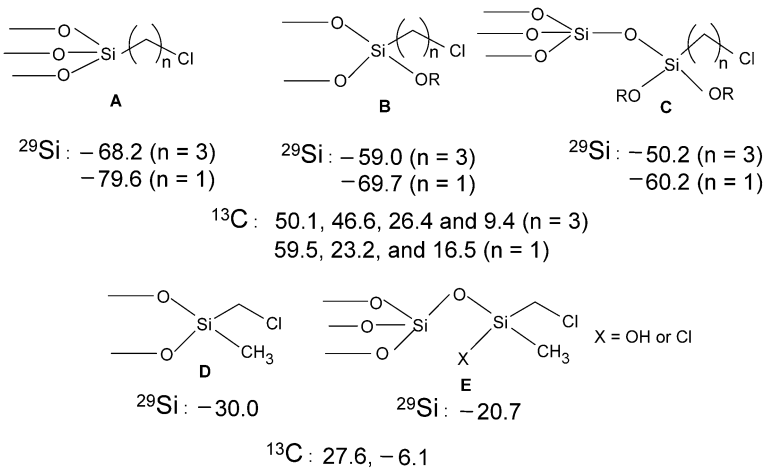

Fig. 2. Schematic formulations of the surface functional groups generated by the treatment of MCM-41 with the silicon reagents.

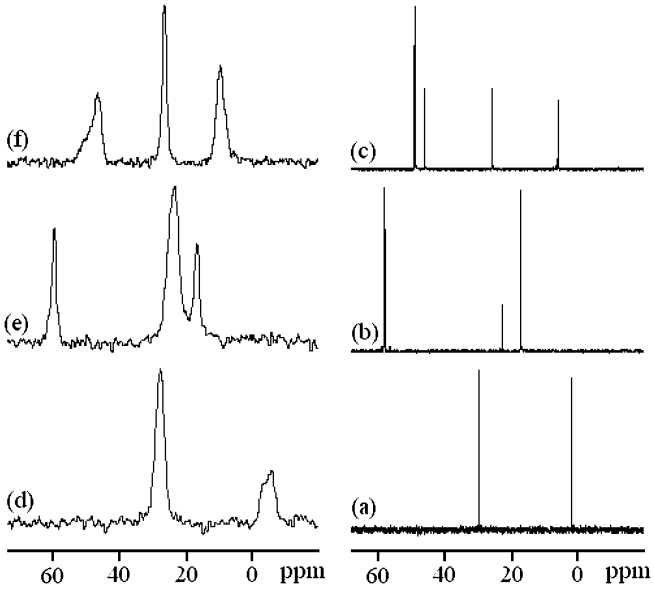

Fig. 3. ^{13}C NMR spectra of neat reagents in solution (a–c) and CPMAS of functionalized MCM-41 (d–f). (c) $(CH_3O)_3SiCH_2CH_2CH_2Cl$; (f) MCM-41 functionalized by $(CH_3O)_3SiCH_2CH_2CH_2Cl$; (b) $(C_2H_5O)_3SiCH_2Cl$; (e) MCM-41 functionalized by $(C_2H_5O)_3SiCH_2Cl$; (a) $(CH_3)Cl_2SiCH_2Cl$; (d) MCM-41 functionalized by$(CH_3)Cl_2SiCH_2Cl$.

(Figs. 3a and 3d) for $Si(CH_3)\mathit{C}H_2Cl$ and $Si(\mathit{C}H_3)CH_2Cl$, respectively.

Finally, because the signals of the host MCM-41 and of the functionalized surface sites are well demarcated in the ^{29}Si MAS spectra, the degree of functionalization in **1′**–**3′** can be determined from the NMR data by spectral deconvulation. Thus, the degree of functionalization with $(CH_3O)_3SiCH_2CH_2CH_2Cl$, $(EtO)_3SiCH_2Cl$, and $(CH_3)Cl_2SiCH_2Cl$ are found to be ∼17, 20, and 11%, respectively. As will be seen later (see Table 4), the NMR-based relative order is in agreement with that based on chemical analysis.

XPS spectra of **1′**–**3′** have been recorded to determine whether there are notable differences between the electronic environments of the surface silicon from MCM-41 and the spacer group functionalized surface silicon ions. Only one Si 2*p* peak at a binding energy (BE) 103.25 eV is observed for **1′** (see Fig. 4a). This core-level signature is indistinguishable from that of **1a** (and MCM-41), indicating that the XPS detectable electronic environments of the silicon on the functionalized surface sites and that of MCM-41 are practically identical. Similar observations are also made for **2′**. The only difference in this case is that the BE of Si 2*p* shifts marginally to 103 eV. This slight difference in the BE of **1′** and **2′** is most likely due to the length of the spacer group. In **1′** there are three carbon atoms between the silicon and the chlorine, compared with only one carbon atom in **2′**.

Table 4
Bulk chemical analysis[a]

Catalyst	Chloroalkyl groups[a] (mmol/g)	Quaternary ammonium group[a] (mmol/g)	Bulk platinum[b] (wt%)
1a	2.1	0.4	4.5
2a	3.7	1.0	5.2
3a	1.3	0.8	5.1
1b	2.0	0.6	5.6
2b	3.4	0.5	4.2
3b	1.4	0.8	5.2

[a] Estimated via elemental (C, H, N) analysis.
[b] Estimated by ICP-AES.

In contrast, there are significant differences between the spectra of **3′** and those of **1′** and **2′**. For **3′**, the Si 2*p* signal can be deconvoluted into two signals at the BE of 102.7 and 103.8 eV; these two signals are attributed to the silicon of functionalized and unfunctionalized surface sites, that is, $(-O)_2Si(CH_3)CH_2Cl$ and MCM-41, respectively. The difference between **3′** on the one hand and **1′** and **2′** on the other hand can also be seen in the valence band spectra (Fig. 4b). XPS features of **3′** shows a rigid shift of 0.5 eV toward higher BE compared with those of **1a**, **1′**, and **2′**, and the same reflects in the valence band and Si 2*p* core level.

Transmission electron micrographs of fresh **1a**, **2a**, and **3a** are shown in Figs. 5a–5c. The characteristic fringes typical of MCM-41 are clearly seen in the micrographs of all of the samples. Note that these are the final catalysts after loading spacer group, NEt_3 and Pt, which clearly hints that the integrity of

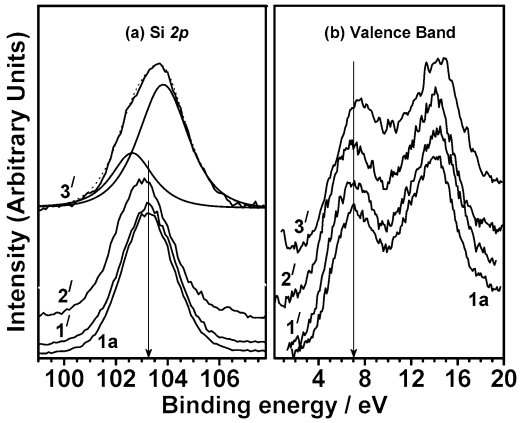

Fig. 4. X-ray photoemission spectra of (a) Si 2*p* core level and (b) valence band of functionalized MCM-41 catalysts before loading NEt_3 and Pt. Results from Pt-loaded MCM-41 are compared to show an excellent agreement with CPTMS functionalized surface and the comparable electronic structure.

MCM-41 is fully retained until the last stage in all three samples. Platinum crystallites are well dispersed and located in the pores of MCM-41. These crystallites must be smaller (<3 nm) than the fringe width (3.5 nm), and because of this they are not observed except for some line broadening at some of the fringe spots (Fig. 5).

3.2. *Spectroscopic and other physicochemical data of **1a–3b***

As reported by us earlier, freshly prepared **1a** and **1b** have IR (2060 and 1850 cm^{-1}) and UV–vis (reflectance, 620 nm) bands that match well with the band of $[Pt_{12}(CO)_{24}]^{2-}$ [14,17]. However, the CO ligands are lost very quickly even when they are stored under CO [14,21]. Similar observations are made for the other four catalysts, **2a**–**3b**. Thus the spacer groups have no observable effect on the stability of the cluster-supported materials toward CO loss. Thus the formulations shown in the scheme are applicable only to the materials before the CO loss and the use of these materials as catalysts. Note that, depending on the nature of the support, the decarbonylated Chini cluster may retain the cluster framework or undergo aggregation. The former behavior has been observed in zeolite Y; the latter, on MgO [22–24].

Catalyst **1a** has been studied by solid-state NMR (CPMAS, ^{29}Si, ^{13}C, ^{15}N) to validate the presence of quaternary ammonium groups on the support. As can be seen from Fig. 6, in the ^{29}Si spectra, out of the T^1, T^2, and T^3 peaks of **1′** there is substantial decrease of T^1 (**C**). The T^2 (**B**) and T^3 (**A**) environments are nearly equally populated. The reaction of **1′** with NEt_3 is carried out in refluxing toluene for 96 h (see Section 2). Under these conditions, the "Si–OR" linkages of the T^1 and T^2 silicon atoms of **1′** are expected to react with the residual silanol groups of the support and to be converted into "Si–O–Si" linkages. In other words, the conversion of **1′** to **1a** is accompanied by conversion of T^1 and T^2 sites into T^3.

In the ^{13}C NMR of **1a**, new peaks attributable to the quaternary ammonium functionalities can be clearly seen. Apart from the ^{13}C resonances of unreacted $(–O)_3SiCH_2CH_2CH_2Cl$ groups, characteristic new peaks corresponding to $(–O)_3SiCH_2CH_2N(CH_2CH_3)_3^+Cl^-$ and $(–O)_3SiCH_2CH_2CH_2N(CH_2CH_3)_3^+Cl^-$ are observed at 53.8 and 59.3 ppm, respectively. The peaks due to $(–O)_3SiCH_2CH_2CH_2N(CH_2CH_3)_3^+Cl^-$ and $(–O)_3SiCH_2CH_2CH_2N(CH_2CH_3)_3^+Cl^-$ can also be seen respectively at 16.0 and 7.6 ppm. Definitive evidence for the presence of $(–O)_3SiCH_2CH_2CH_2N(CH_2CH_3)_3^+Cl^-$ in **1a** comes from the solid-state natural abundance ^{15}N spectrum (Fig. 6) recorded under CPMAS conditions. The ^{15}N resonance occurs at 24.9 ppm and is very close to the reported value (28.2 ppm) for $NEt_4^+I^-$ [25].

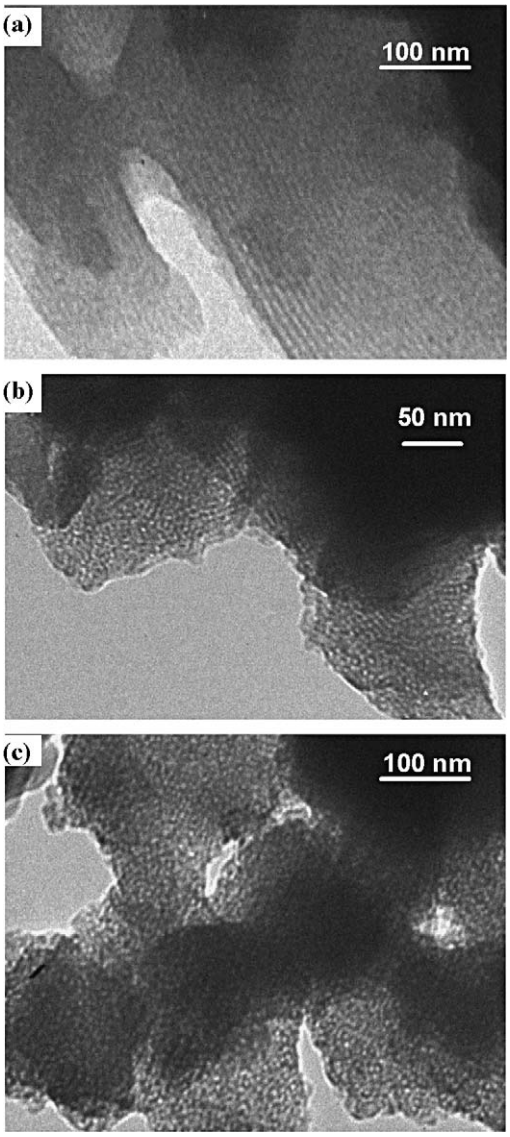

Fig. 5. Transmission electron micrographs obtained from functionalized MCM-41 samples after NEt_3 and Pt loading: (a) **1a**, (b) **2a**, and (c) **3a**.

The extents of incorporation of different functional groups as measured by chemical analysis and other techniques are shown in Table 4. For the MCM-41-based catalyst the order in terms of chloroalkyl content is **2a** > **1a** > **3a**. As mentioned earlier, this order is in agreement with the one based on ^{29}Si NMR data. The chloroalkyl contents of both **3a** and **3b** are notably less than that of the other four catalysts, which indicates

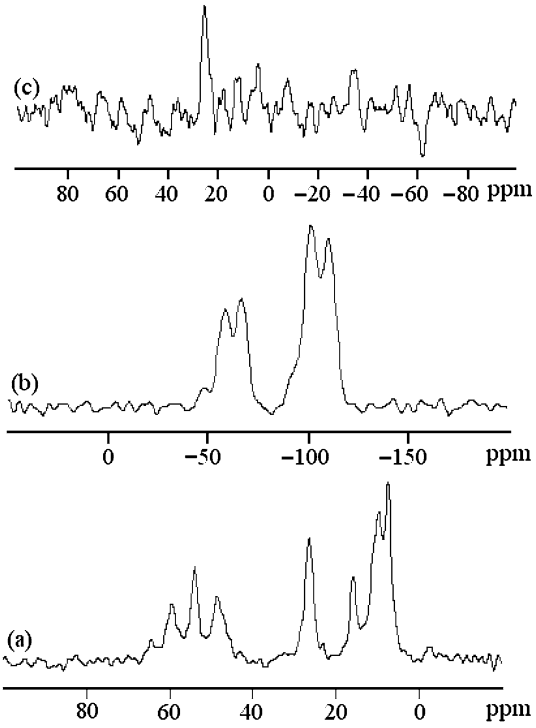

Fig. 6. (a) ^{13}C CPMAS, (b) ^{29}Si CPMAS, and (c) ^{15}N CPMAS spectra of **1a**.

that $(CH_3)Cl_2SiCH_2Cl$ is less reactive than the other two silane reagents.

The observed nitrogen and chloropropyl values indicate that even after the treatment with excess amine a large number of chloroalkyl groups remain unreacted. Consistent with the bulk chloroalkyl content derived from microanalysis, significant amount of chlorine on the surface is also seen by EDAX. Maximum reaction (∼37%) with amine is observed for the supports functionalized by $(CH_3)Cl_2SiCH_2Cl$, but for the other two silane reagents, the extent of reaction is ⩽20%.

*3.3. Catalytic hydrogenation by **1a–3b***

We recently reported the reaction of cinchonidine in place of triethylamine with **1′**, to give a support that has chiral pendant groups [13]. Under optimum conditions, the cluster-derived catalyst from such a support exhibits good enantioselectivity in the hydrogenation of methyl pyruvate and acetophenone [21]. In view of this, attempts were made to react **2′** and **3′** with cinchonidine. Interestingly, under the conditions where **1′** reacts with cinchonidine, no reaction is observed with **2′** and **3′**. The separation of the chlorine atom from the surface by a three-carbon chain thus seems to be essential for any reaction with a bulky amine, such as cinchonidine.

It is important to note that the total numbers of carbon, nitrogen, and oxygen atoms in cinchonidine are 19, 2, and 1, whereas in triethylamine they are 6, 1, and 0, respectively. This observation (i.e., the critical dependence of the reactivity of **1′–3′** on the length of the spacer group), as well as the steric bulk and/or shape of the incoming reactant, guided our catalytic studies described below.

Using **1a–3b** as catalysts, preliminary data on the hydrogenation of ketones, ketoesters, and benzonitrile were obtained (Table 1). We chose these substrates because we had previously reported data some on them with similar cluster-derived catalytic systems [13,14,21]. Control experiments also established that in solution, in the presence or absence of triethylamine, $[Pt_{12}(CO)_{24}]^{2-}$ as a homogeneous catalyst has zero activity for hydrogenation of all of the substrates listed in Tables 1–3. As can be seen from Table 1, for all of the substrates, the highest turnover numbers are obtained with **1a**, indicating that MCM-41, when functionalized with the silane reagent containing the "chloropropyl" group rather than the "chloromethyl" group, yields the most active catalyst.

We previously reported and discussed in detail the TEM and ESCA data on **1a** [13,21]. On ESCA, two signals were observed for platinum $4f$; these were assigned to the decarbonylated platinum cluster and a Pt^{2+} species, probably $PtCl_2$, at a ratio of approximately 10:1. TEM studies of used **1a** had shown platinum crystallites of 5–15 nm that appeared to gather at the edges of the MCM-41 support. Similar observations are also made for **2a** and **3a**. Thus, insofar as the nature of the cluster-derived active sites of **1a**, **2a**, and **3a** are concerned, no significant and systematic differences were observed by ESCA or TEM techniques of resolving power specified in Section 2.

Therefore, the superior activity of **1a** compared with the other five catalysts must be due in part to the higher surface area of MCM-41 (∼600–750 m^2/g) compared with fumed silica (∼180–300 m^2/g) and in part to the longer spacer group. Note that among the fumed silica-based catalysts, **1b** is more active than **2b** and **3b**, again indicating that a longer spacer group gives higher turnovers.

To keep the focus on the effect of the spacer group, extensive turnover data keeping MCM-41 as the support were obtained. Thus, **1a–3a** were used as hydrogenation catalysts for various substrates under a range of reaction conditions (Tables 2 and 3). However, for a given substrate, the reaction conditions were the same for all three catalysts. In other words, for a given substrate, major differences in catalytic activity (turnovers) could be reasonably ascribed to the differing natures of the interactions between the spacer groups and the substrate.

As can be seen from Tables 2 and 3, for every substrate, the highest turnovers were obtained with **1a** as the catalyst. This is true for the hydrogenation of functional groups as disparate as those of ketones, ketoesters, nitroaromatics, alkenes, and nitrile. A longer spacer group would be expected to decrease the steric and/or diffusional interaction between the incoming reactants and the active sites, which, as observed, should result in superior activity.

This plausible explanation is further supported by comparing the activities of the catalysts for any two substrates with the same functional group but different steric bulk and/or shape. Thus, as shown in Fig. 7, in all cases for a given functional group, the reduction in turnover for both **2b** and **3b** is significantly greater for substrates with greater steric bulk.

Because the total number of atoms is the same in both acetophenone and cyclohexanone, their steric bulk may be considered approximately equal. However, the reductions in turnovers

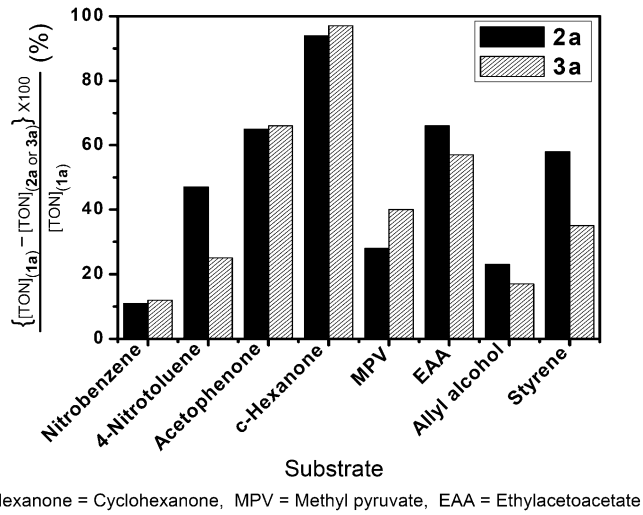

Fig. 7. Decrease (%) in TON of **2a** and **3a** with respect to TON of **1a**.

for **2a** and **3a** are 65 and 66% for acetophenone, compared with 94 and 97% for cyclohexanone. The nonplanarity of cyclohexanone, in contrast to the planarity of the aromatic ring of acetophenone, probably leads to hindrance that is mainly stereoelectronic (i.e., shape-dependent), and, consequently, the turnovers are reduced.

Therefore, the turnover data given in Tables 1–3 are in good agreement with the conjecture that the length of the spacer group primarily determines the steric- and/or shape-dependent interaction between the incoming reactants and the active sites, and has a direct correlation with the observed activity. But this does not mean that there may not be other differences (e.g., structural, electronic) among the active sites of the three catalysts. Such differences are likely in view of the different types of functional groups identified by NMR for **1a** and **2a** on the one hand and **3a** on the other hand. The notably different activities of **2a** and **3a** for 4-nitrotoluene, cyclohexanone, and styrene are probably indicative of such differences.

4. Conclusion

The T^1, T^2, and T^3 sites of MCM-41 functionalized with $(EtO)_3SiCH_2Cl$, $(MeO)_3SiCH_2CH_2CH_2Cl$, and $(CH_3)Cl_2SiCH_2Cl$ were fully characterized by solid-state NMR (CPMAS, ^{29}Si, and ^{13}C). The electronic environments of functionalized sites were also explored by XPS. After further functionalization with triethylamine, these materials were used as inorganic anion exchangers to support the cluster anion $[Pt_{12}(CO)_{24}]^{2-}$. Solid-state NMR (^{29}Si, ^{13}C, ^{15}N) of the resultant materials established the presence of the quaternary ammonium groups, whereas TEM showed that the basic structure of MCM-41 was maintained. Analogous materials were also produced with fumed silica as the support. Comparative catalytic hydrogenation studies on ketones, nitroaromatics, alkenes, and benzonitrile were carried out with these six precatalysts. The best activities were obtained for the catalyst with chloropropyl as the spacer group. Analysis of the turnover data indicated that steric interaction between the spacer group and the incoming substrate played a critical role in determining activity.

Acknowledgments

Financial assistance from Reliance Industries Limited, Mumbai, India and the Council of Scientific and Industrial Research, New Delhi, India is gratefully acknowledged.

References

[1] M. Lemaire, Pure Appl. Chem. 76 (2004) 679.
[2] P. McMorn, G.J. Hutchings, Chem. Soc. Rev. 33 (2004) 108.
[3] D.E. Bergbreiter, Chem. Rev. 102 (2002) 3345.
[4] J.A. Gladysz, Chem. Rev. 102 (2002) 3215.
[5] C.A. McNamara, M.J. Dixon, M. Bradley, Chem. Rev. 102 (2002) 3275.
[6] C.E. Song, S. Lee, Chem. Rev. 102 (2002) 3495.
[7] N.E. Leadbeater, M. Marco, Chem. Rev. 102 (2002) 3217.
[8] T. Shimada, K. Aoki, Y. Shinoda, T. Nakamura, N. Tokunaga, S. Inagaki, T. Hayashi, J. Am. Chem. Soc. 125 (2003) 4688, and references cited therein.
[9] C.D. Nunes, A.A. Valente, M. Pillinger, A.C. Fernandes, C.C. Romão, J. Rocha, I.S. Gonçalves, J. Mater. Chem. 12 (2002) 1735.
[10] C.D. Nunes, M. Pillinger, A.A. Valente, I.S. Gonçalves, J. Rocha, P. Ferreira, F.E. Kühn, Eur. J. Inorg. Chem. 5 (2002) 1100.
[11] T.M. Jyothi, M.L. Kaliya, M. Herskowitz, M.V. Landau, Chem. Commun. (2001) 992.
[12] S. Abramson, N. Bellocq, M. Laspéras, Top. Catal. 13 (2000) 339.
[13] S. Basu, H. Paul, C.S. Gopinath, S. Bhaduri, G.K. Lahiri, J. Catal. 229 (2005) 298.
[14] H. Paul, S. Bhaduri, G.K. Lahiri, Organometallics 22 (2003) 3019.
[15] E.J.R. Sudhölter, R. Huis, G.R. Hays, N.C.M. Alma, J. Colloid Interface Sci. 103 (1985) 554.
[16] J.S. Beck, J.C. Vartulli, W.J. Roth, M.E. Leonowicz, C.T. Kresge, K.D. Schmitt, C.T.-W. Chu, D.H. Olson, E.W. Sheppard, S.B. McCullen, J.B. Higgins, J.L. Schlenker, J. Am. Chem. Soc. 114 (1992) 10834.
[17] G. Longoni, P. Chini, J. Am. Chem. Soc. 98 (1976) 7225.
[18] M. Jia, A. Seifert, W.R. Thiel, Chem. Mater. 15 (2003) 2174.
[19] M. Pillinger, I.S. Gonçalves, A.D. Lopes, J. Madureira, P. Ferreira, A.A. Valente, T.M. Santos, J. Rocha, J.F.S. Menezes, L.D. Carlos, Dalton Trans. 10 (2001) 1628.
[20] C. Venkatesan, A.P. Singh, Stud. Surf. Sci. Catal. 154 (2004) 2795.
[21] S. Basu, M. Mapa, C.S. Gopinath, M. Doble, S. Bhaduri, G.K. Lahiri, J. Catal. 239 (2006) 154.
[22] J.G.-C. Shen, J. Phys. Chem. B 104 (2000) 423.
[23] G. Sastre, N. Raj, C.R.A. Catlow, R. Roque-Malherbe, A. Corma, J. Phys. Chem. B 102 (1998) 3198.
[24] J.-R. Chang, D.C. Koningsberger, B.C. Gates, J. Am. Chem. Soc. 114 (1992) 6460.
[25] T. Giavani, K. Johannsen, C.J.H. Jacobsen, N. Bolm, H. Bildsøe, J. Skibsted, H.J. Jakobsen, Solid State Nucl. Magn. Reson. 24 (2003) 218.